# A magnetotactic bacteria-based biorefinery: Potential for generating multiple products from a single fermentation

| | |
|---|---|
| Journal: | *ACS Sustainable Chemistry & Engineering* |
| Manuscript ID | sc-2021-02435z.R3 |
| Manuscript Type: | Article |
| Date Submitted by the Author: | n/a |
| Complete List of Authors: | Hierro-Iglesias, Carmen; Aston University School of Engineering and Applied Science, Chemical Eng & Applied Chemistry<br>Masó-Martínez, Marta; Aston University School of Engineering and Applied Science, Chemical Eng & Applied Chemistry<br>Dulai, Jugraj; Aston University School of Engineering and Applied Science, Chemical Eng & Applied Chemistry<br>Chong, Katie; Aston University, European Bioenergy Research Institute<br>Blanco-Sanchez, Paula; Aston University, Chemical Engineering & Applied Chemistry<br>Fernandez-Castane, Alfred; Aston University School of Engineering and Applied Science, Chemical Eng & Applied Chemistry |
| | |

# A magnetotactic bacteria-based biorefinery: Potential for generating multiple products from a single fermentation

Carmen Hierro-Iglesias[1,±], Marta Masó-Martínez[1,±], Jugraj Dulai[1], Katie J Chong[1], Paula Helena Blanco-Sanchez[1], Alfred Fernández-Castané[1,*]

[1]Energy and Bioproducts Research Institute & Aston Institute of Materials Research, Aston University, Birmingham, B4 7ET, UK

Carmen Hierro-Iglesias (CHI) 190217633@aston.ac.uk

Marta Masó-Martínez (MMM) 200193447@aston.ac.uk

Jugraj Dulai (JD) dulaij@aston.ac.uk

Katie J Chong (KC) k.chong1@aston.ac.uk

Paula Helena Blanco-Sanchez (PBS) p.blanco-sanchez@aston.ac.uk

Alfred Fernández-Castané (AFC) a.fernandez-castane1@aston.ac.uk

[±] These authors contributed equally

## ABSTRACT

The magnetotactic bacteria model *Magnetospirillum gryphiswaldense* MSR-1 (*Mgryph*) is typically known for its capacity to produce magnetic nanoparticles with unique properties, namely magnetosomes. However, the magnetosome fraction represents only around 4% of the total cell mass. Therefore, the downstream processing of *Mgryph* generates a substantial amount of under-utilised microbial biomass waste (MBW) rich in proteins and polyhydroxyalkanoates (PHA), which can be used, for example, as animal feed and biodegradable bioplastics, respectively.

In this work, we have designed an integrated *Mgryph*-based biorefinery through the utilisation of the MBW for the recovery of PHA and soluble proteins using NaClO extraction, revealing that poly(3-hydroxybutyrate-co-3-hydroxyvalerate) is produced with a relative abundance of 99:1 mol% (3HB:3HV). We have further upgraded PHA into crotonic acid using pyrolysis, which can be used in adhesives and biofuels manufacturing. The effect of the MBW concentration used in the NaClO extraction step (10, 30 and 50 g MBW·L$^{-1}$) was evaluated to determine PHA recovery yields, purity and purification factor, as well as the thermal stability and fraction of volatile components. The condition using 10 g MBW·L$^{-1}$ was the best among those tested with 51.3 ± 0.14% polyhydroxyalkanoates (PHA) content in the extract, 97.8% extraction yield and 2.93 purification factor. The thermogravimetric analysis of PHA extracts from *Mgryph* showed a degradation range between 232 – 292°C and a purity of up to 73 ± 4%. Under optimal extraction conditions (10 g MBW·L$^{-1}$), 53.3% of the total cellular protein was recovered. Analysis of products from isothermal pyrolysis of PHA extracts at 300°C yielded up to 86.0 ± 1.5% of crotonic acid.

To the best of our knowledge, our study is the first to extract PHA from *Mgryph*, thus representing a benchmark for future optimization studies for PHA recovery in this microorganism. Moreover, this work explores the development of an integrated *Mgryph*-based

biorefinery for valorising microbial biomass waste into added value biochemicals, which can be used in a wide range of applications, thus representing an opportunity to improve the efficiency of magnetosome production towards the development of sustainable bioprocesses.

**KEYWORDS**

Valorisation, Sustainable biomanufacturing, Green technology, Clean bioprocessing, microbial waste biomass, *Magnetospirillum gryphiswaldense* MSR-1, polyhydroxyalkanoates, crotonic acid, magnetosomes

## INTRODUCTION

It is expected that by 2050, the bioeconomy will represent up to 10% of global industrial production, corresponding to €23 Trillion [1]. Bio-technologies, offer a huge potential to impact the bioeconomy to mitigate climate change by developing greener, cleaner manufacturing processes and new products that benefit society through the use of living organisms.

Microbial biotechnologies developed in biorefinery processes include algae for biofuels production [2], bacteria for the recovery of metals from e-waste [3] and mixed microbial communities in anaerobic digestion (AD) [4]. Moreover, microbes are also used for industrial biotechnology (IB) applications to produce bio-based products such as enzymes [5] and fine chemicals [6]. Manufacturing of bio-based products generally entails the need for downstream (recovery and purification) processing. As a result, a significant fraction of microbial biomass is generated in industrial fermentations as waste. The microbial biomass waste (MBW) is a nutrient-rich organic stream that contains by-products that offer the potential for valorisation for agricultural use [7] or animal feed [8]. Therefore, future challenges that the bioeconomy must address include developing more efficient industrial processes with a low carbon footprint; offering circular economy solutions with minimal waste generation.

The subject of this study, magnetotactic bacteria (MTB), are well known because they make tiny crystals of iron called magnetosomes [9], which are "nanomagnets" that can be used as an innovative alternative to traditional chemical magnetic nanoparticles (MNPs) due to their advantageous and unique properties: they are ferrimagnetic; have a narrow size distribution; are wrapped in a phospholipid bilayer membrane containing a unique set of specific proteins, preventing aggregation; and can be functionalized through chemical or genetic modification, the latter allowing one-step manufacture [10]. Their applications in the healthcare arena include, for example, cancer treatment [11,12], MRI contrast agents [13,14] and antimicrobials [15,16]. Therefore, magnetosomes have the potential to become the next generation of nanomedicines produced

using biological and environmentally friendly routes. Recent advances in MTB research have shown that MTB can be used in environmental and bioenergy applications, such as electricity generation [17], bioremediation [18,19] and e-waste valorisation [20].

*Magnetospirillum gryphiswaldense* (*Mgryph*) is the most widely studied MTB model and offers great potential for industrial applications due to the understanding of its genetics [21,22] and physiology [23]; and the availability of toolboxes for genetic manipulation [24]. Recent bioprocessing works have reported cell densities of *Mgryph* in bioreactor cultivation of 9.16 g DCW·$L^{-1}$ [25], 4.2 g DCW·$L^{-1}$ [26] and 2.4 g DCW·$L^{-1}$ [27] with yields of magnetosomes of 356.52 mg·$L^{-1}$, 53.5 mg·$L^{-1}$ and 10 mg·$L^{-1}$, respectively. *Mgryph* has limited capacity to form magnetosomes as it generates up to 4% of its dry weight as magnetosomes [28].

Genetic modifications have enabled increased magnetosome production. By overexpressing the genes implicated in the synthesis of magnetosomes located in a conserved genomic magnetosome island (MAI), magnetosome production was increased 2.2-fold compared to the wild type [29]. Purification of magnetosomes generally encompasses a cell disruption step followed by magnetic separation [30]. This process can be quite lengthy and tedious if manual "washings" are employed [31]. In contrast, semi-automated procedures for magnetosome recovery have been developed, resulting in more efficient and shorter downstream processing (DSP) [32]. Regardless of the DSP approach used for magnetosome recovery, large volumes of residual *Mgryph* lysate are produced and disposed of, accounting for around 96% of the total DCW.

Recent work carried out in our research group has found that varying amounts of polyhydroxyalkanoates (PHA) and magnetosomes are formed in bioreactor experiments [26]. PHA are a family of biodegradable and biocompatible polymers that present promising applications for packaging or as drug carriers [33]**.** Notably, excessive reducing power in *Mgryph* fermentations is consumed through polyhydroxyalkanoates (PHA) synthesis and hydrogen

release in MTB [34]. This process may be explained to some extent because MTB produces PHA granules constitutively that act as nutrient storage [28]**.** Furthermore, recent works demonstrate an energy competition between the process formation of PHA and magnetosomes [35]. Interestingly, PHA can be upgraded using pyrolysis technology to produce crotonic acid [36], an optically-active polymer traditionally produced from non-renewable resources and can be used as a chemical platform for the synthesis of copolymers [37] or as enrichment of bio-oils [38]. Upon downstream processing of *Mgryph*, PHA are found as part of the residual biomass after magnetosome purification. Hence, *Mgryph* can be exploited as a microbial factory capable of synthesising two valuable *materials* that can be used for multiple applications.

In this work, we evaluate the potential of *Mgryph* for the development of magnetotactic bacteria-based biorefineries for generating multiple products from a single fermentation. We have used the MBW generated after magnetosome purification to recover and characterise PHA and determine the amount of soluble protein after applying aqueous two-phase extraction with NaClO. Additionally, we have employed pyrolysis on extracted PHA for the production of crotonic acid.

## MATERIALS AND METHODS

### Strains, media and culture conditions

*Magnetospirillum gryphiswaldense* MSR-1 (*Mgryph*) was obtained from Deutsche Sammlung von Mikroorganismen und Zellkulturen GmbH (DSMZ, Germany) and used for all experiments. Unless indicated otherwise, all chemicals were purchased from Fisher (Loughborough, UK). Cryostocks of *M. gryphiswaldense* in 5% DMSO were routinely grown in flask standard medium (FSM) comprising: 3.5 $g \cdot L^{-1}$ potassium l-lactate; 100 µM iron citrate ($C_6H_5FeO_7$); 0.1 $g \cdot L^{-1}$ $KH_2PO_4$; 0.15 $g \cdot L^{-1}$ $MgSO_4 \cdot 7H_2O$; 2.38 $g \cdot L^{-1}$ HEPES; 0.34 $g \cdot L^{-1}$ $NaNO_3$; 0.1 $g \cdot L^{-1}$ yeast extract; 3 $g \cdot L^{-1}$ soy bean peptone; and 5 $mL \cdot L^{-1}$ EDTA-chelated trace

element solution (EDTA-TES; [39]). EDTA-TES contained: 5.2 g·L$^{-1}$ EDTA disodium salt; 2.1 g·L$^{-1}$ $FeSO_4 \cdot 7H_2O$; 30 mg·L$^{-1}$ $H_3BO_3$; 85.4 mg·L$^{-1}$ $MnSO_4 \cdot H_2O$; 190 mg·L$^{-1}$ $CoCl_2$ g·L$^{-1}$; 4 mg·L$^{-1}$ $NiCl_2 \cdot 6H_2O$; 2 mg·L$^{-1}$ $CuCl_2 \cdot 2H_2O$; 44 mg·L$^{-1}$ $ZnSO_4 \cdot 7H_2O$ and 36 mg·L$^{-1}$ $Na_2MoO_4 \cdot 2H_2O$. Pre-cultures used for bioreactor inoculation were grown in FSM without an iron source. The pH of FSM was adjusted to 7.0 with NaOH. Cells were grown at 30°C in flat-bottomed flasks in an orbital shaker incubator Incu-Shake MAXI® (SciQuip Ltd, Newtown, UK) operated at 150 rpm.

The batch medium for bioreactor experiments is as described elsewhere [26] and the feed solution contained: 100 g·L$^{-1}$ lactic acid; 25 g·L$^{-1}$ $NaNO_3$; 18 mL·L$^{-1}$ 25 – 28% $NH_3 \cdot H_2O$; 6 g·L$^{-1}$ yeast extract; 2.4 g·L$^{-1}$ $MgSO_4 \cdot 7H_2O$; 6 g·L$^{-1}$ $K_2HPO_4 \cdot 3H_2O$; 70 mL·L$^{-1}$ Mineral Elixir and 2 g·L$^{-1}$ $FeCl_3 \cdot 6H_2O$. The mineral elixir (pH 7) contained: 1.5 g·L$^{-1}$ nitrilotriacetic acid; 3 g·L$^{-1}$ $MgSO_4 \cdot 7H_2O$; 0.5 g·L$^{-1}$ $MnSO_4 \cdot 2H_2O$; 1 g·L$^{-1}$ NaCl; 0.1 g·L$^{-1}$ $FeSO_4 \cdot 7H_2O$; 0.18 g·L$^{-1}$ $CoSO_4 \cdot 7H_2O$; 0.1 g·L$^{-1}$ $CaCl_2 \cdot 2H_2O$; 0.18 g·L$^{-1}$ $ZnSO_4 \cdot 7H_2O$; 0.01 g·L$^{-1}$ $CuSO_4 \cdot 5H_2O$; 0.02 g·L$^{-1}$ $KAl(SO_4)_2 \cdot 12H_2O$; 0.01 g·L$^{-1}$ $H_3BO_3$; 0.01 g·L$^{-1}$ $Na_2MoO_4 \cdot 2H_2O$; 0.03 g·L$^{-1}$ $NiCl_2 \cdot 6H_2O$ and 0.3 mg·L$^{-1}$ $Na_2SeO_3 \cdot 5H_2O$.

Bioreactor set up

A Biostat B (Sartorius Stedim UK Ltd, Surrey, UK) with a 1-L jacketed bioreactor equipped with four baffles and an agitator with 2 six-bladed Rushton turbines was used. Aeration was achieved by sparging a mixture of air/nitrogen (1:2) from below the lower impeller at a rate of 50 – 150 mL·min$^{-1}$ through a reusable, autoclavable 0.22-µm filter (Sartorius). Dissolved oxygen in the medium ($pO_2$) was measured online using an Oxyferm FDA VP 325 (Hamilton, Bonaduz, Switzerland). Agitation was maintained at 150 – 500 rpm. pH was measured using an EasyFerm Plus PHI VP 325 Pt100 (Hamilton, Bonaduz, Switzerland) and was controlled at a set-point of 7 ± 0.05 with the automated addition of an acidic feeding solution. Off-gas passed

through a condenser, autoclavable 0.22-µm filter (Sartorius, Goettingen, Germany) and HEPA filter (Millipore, Darmstadt, Germany). The temperature was maintained at 30°C by heating the water in the jacket.

Cell disruption and magnetosome purification

730 mL of *Mgryph* broth at the mid-exponential phase, which corresponds to an $OD_{565}$ ~ 5.9 (14.35 g WCW (wet cell weight) /L)were harvested using a Heraeus Multifuge X1R centrifuge (Thermo Scientific, Massachusetts, USA)) at 4,000 for 20 min, with temperature control set at 4ºC. The supernatant was discarded and cells were stored at -18ºC for further use. Subsequently, cells (8 g WCW) were thawed at 4°C and suspended in 20 mL of homogenization buffer (50 mM HEPES buffer 4mL EDTA pH 7.4) at a final concentration of 32% wet cell weight (w/v), making up a "*Mgryph* homogenized" solution of c.a. 25 mL. Cells were disrupted using a Probe sonicator (Fisherbrand™ Model 120 Sonic Dismembrator, Fisher Scientific, Loughborough, UK) operation at 20 kHz and 70% amplitude (power). Sonication was carried out with 1 sec on / 1 sec off pulses for 20 min. Magnetosomes from sonicated samples were partially purified using a single '60 × 30 × 15' mm NdFeB magnet (Q-60-30-15-N, Supermagnete) placed against vertically positioned 50 mL falcon tubes containing 20 mL homogenate by 9 sequential washes with 20 mL of "wash" buffer (10 mM HEPES 4mM EDTA, pH 8). Magnetosomes were finally resuspended in 6 mL of wash buffer. A further purification step followed partial purification by layering magnetosome samples onto a 60% sucrose cushion in 10 mM HEPES 4mM EDTA buffer pH 8.0 and ultracentrifuged (Optima™ TLX Ultracentrifuge, Beckman Coulter) at 100,000 $g_{av}$ using a TLA-120.2 Rotor (Beckman Coulter) for 2.5 h at 4°C. Pure magnetosomes were resuspended in 10 mM HEPES 4mM EDTA buffer pH 8.0 before analysis, whereas "wash" fractions were pulled together, mixed gently to homogenise and stored -18ºC until further analysis.

Extraction of polyhydroxyalkanoates by sodium hypochlorite digestion

The protocol developed by Heinrich and co-workers [40] was adapted to extract PHA from *Mgryph*. The "Wash" pool containing the cell debris was freeze-dried (VirTis 4K, SP Industries, PA, USA). Subsequently, the pulverised cell debris was weighed using an analytical balance (ABJ-NM, KERN & SOHN GmbH, Balingen, Germany). Following freeze-drying, pulverised cells (10, 30 and 30 $g \cdot L^{-1}$) were suspended in an aqueous 13% (w/v) sodium hypochlorite solution (NaClO) with a pH of 11.8 and incubated at room temperature for 1 h. Then, $dH_2O$ was added to make up a 50% increase of volume to enhance the PHA sedimentation rate, incubated at room temperature, standing for 8 h. The upper phase (containing water-soluble components) was removed and stored at -18$^{o}$C until further analysis. The bottom phase (containing PHA) was washed twice by centrifugation (Thermo Scientific Heraeus Multifuge X1R) for 10 minutes at 4000 $g_{av}$ at 4$^{o}$C with an equal volume of $dH_2O$ and resuspended with 2 mL isopropanol. Subsequently, the solution was freeze-dried (VirTis 4K, SP Industries, PA, USA), weighed using an analytical balance (ABJ-NM, KERN & SOHN GmbH, Balingen, Germany) and stored at room temperature in a desiccator with silica gel beads until further analysis.

Analytical procedures

Cell growth

*Mgryph* optical density at 565 nm ($OD_{565}$) was measured using a spectrophotometer (Evolution 300 UV-Vis, Thermo Scientific, UK). Data were collected using VISIONpro software. One $OD_{565}$ is equivalent to 0.28 g dry cell weight (DCW) per $L^{-1}$ [26].

Iron content

Inductively coupled plasma optical emission spectroscopy (ICP-OES, Thermo Scientific iCAP 7000) coupled to a Teledyne CETAC ASX-520 Random Access Autosampler was used as an offline analysis to study the intracellular iron concentration of magnetosomes preparations. Iron concentration was determined at a wavelength of 259.94 nm. Sample preparation was completed in triplicate as described elsewhere [41]. Briefly, 500 µL nitric acid (70% v/v) was used to solubilize the iron in the form of magnetite pellets and incubated at 98°C for 2 h with shaking at 300 rpm.

Fluorescence analysis

Before pulling all "wash" fractions together, fluorescent spectroscopy was carried out for the nine "wash" fractions using an F-2500 fluorescence spectrophotometer (Hitachi High-Technologies Corporation, Japan) equipped with a Xenon arc lamp. One mL of "wash" was pelleted down at 13,300 $g_{av}$ for 5 min using an AccuSpin Micro 17 centrifuge (Thermo Fisher Scientific, Massachusetts, USA). The supernatant was discarded, and the pellet was resuspended with an equal volume of $dH_2O$. Ten µL of the lipid-binding fluorophore pyrromethene-546 (Pyr-546, CAS 121207-31-6, Merck) 0.1 $mg \cdot mL^{-1}$ in dimethyl sulfoxide were added prior to analysis. The relative fluorescence intensity (RFI) of Pyr-546 was measured at an excitation wavelength (i.e., activating wavelength, $\lambda_{exc}$) of 480 nm and an emission wavelength (i.e., fluorescence wavelength, $\lambda_{em}$) of 540 nm at room temperature. Fluorescence spectra were acquired between 200 and 800 nm. The slit width for excitation and emission was kept to 10 nm. The photo-multiplier tube voltage was set at 400 V. In parallel, 100 µL of each "wash" fraction was directly stained with 5 µL of 0.1 $mg \cdot mL^{-1}$ pyrromethene-546 (Pyr-546) in dimethyl sulfoxide for polyhydroxyalkanoates (PHA) imaging and vortexed for 5 seconds. A Zeiss Primo Star iLed microscope (Carl Zeiss Ltd., Cambridge, UK) fitted with a Zeiss AxioCam ERc 5s camera was used. Images were acquired within 2 min

of fluorophore incubation using x100 lenses and oil immersion and processed with Zeiss ZEN Lite 2012 software in auto exposure mode. Samples were excited with a Zeiss Led 470 nm light source, and a 515 LP filter was employed to detect Pyr-546 fluorescence.

Gas chromatography-mass spectrometry

Poly(3-hydroxybutyrate-co-3-hydroxyvalerate) (P(3HB-co-3HV)) copolymer content was determined from PHA extracts using Gas chromatography-mass spectrometry (GC-MS). The propanolysis method was adapted from elsewhere [42] with 5 mg of lyophilized PHA extract in 2 mL of chloroform and 2 mL of 1-Propanol containing 25% of 37% (v/v) HCl. One-hundred µL of 1 mg·mL$^{-1}$ benzoic acid in 1-propanol was added as an internal standard. Subsequently, mixtures were incubated for 2 h at 100°C in Pyrex glass tubes with a screw cap and cooled down to room temperature. Next, 4 mL of $dH_2O$ was added, the tube was vortexed for 30 s and left for 5 min for phase separation. The upper aqueous phase was removed, and 4 mL of $dH_2O$ was added to the bottom phase, vortexed and left for phase separation as in the previous step. The aqueous phase was discarded. One mL of the organic phase was filtered using 0.22 µm syringe filters (Millipore) and transferred into a GC-MS vial for analysis. 3-hydroxybutyric acid (3HB, Acros Organics, CAS num 300-85-6) and (P(3HB-co-3HV)) copolymer (3HV 8 mol%) (3HV, Merck, CAS num 80181-31-3) were used as standards. Samples were prepared in triplicate. The analysis was performed using a gas chromatograph (Trace 13000) equipped with a 30 m Agilent column (122-0712, DB-1701) at 280°C and coupled to a single quadruple mass spectrometer (ISQ LT). One µL of the sample was injected. The flow rate was set at 1.25 mL·min$^{-1}$ and the ionization detector at 240°C. The column temperature was programmed from 40°C to 250°C at a rate of 5°C·min$^{-1}$. The components of interest were investigated using the internal libraries *nist_msms* and *replip*. The 3HB content in PHA was calculated by

interpolating the peak intensity with the calibration curve generated using standards. The 3HV content in PHA was calculated as the ratio of 3HV and (3HB + 3HV) monomers (as mol%).

The yield of PHA recovery was calculated as follows:

Yield (%) = (Final PHA mass/Initial PHA mass) x 100 Eq. 1

The PHA purification factor was calculated as follows:

Purification factor (%) = (PHA concentration in extracts/ PHA concentration in *Mgryph* homogenized) x 100 Eq. 2

Thermogravimetric analysis

Thermogravimetric analysis (TGA) was conducted to test the thermal stability of PHA after NaClO extraction was performed in duplicate for each extraction condition. The analysis was conducted using a TGA/DSC 2 analyser (Mettler Toledo, Leicester, UK) in an inert atmosphere with $N_2$. Approximately 5 mg of sample was heated from 20$^{o}$C to 800$^{o}$C at a heating rate of 20$^{o}$C min$^{-1}$. The mass of PHA from *Mgryph* in each sample was determined as the mass loss in the temperature range between 232°C and 274°C (for the untreated, 30 g MBW·L$^{-1}$ and 50 g MBW·L$^{-1}$ extracts) or 294°C (for the 10 g MBW·L$^{-1}$ extract). The mass of commercial PHB was determined as mass loss in the temperature range between 290°C and 325°C.

The purity of PHA was calculated as follows:

$Purity_{TGA}$ (%) = (Mass of PHA/Total mass of sample) x 100 Eq. 3

Protein content

The total protein concentration of the upper phase (obtained upon NaClO extraction of PHA) was determined spectroscopically using the BCA assay kit (ThermoFisher Scientific,

Waltham, MA, USA) as per the manufacturer's instructions. Samples were analysed in duplicate. The yield of protein recovery was calculated as follows:

$Yield\ (\%) =$ (Final protein mass/Initial total protein mass) x 100 Eq. 4

Pyrolysis of polyhydroxyalkanoates extracts

Small scale fast pyrolysis was carried out with PHA extracts after NaClO extraction. Samples were placed in open-ended quartz tubes (~2 mm diameter, 20 mm length). The tubes were loaded with 0.1-0.2 mg of PHA extract with two layers of quartz wool above and below the sample. A Pyroprobe 5200 pyrolyzer (CDS Analytical) coupled to a PerkinElmer Clarus 680 gas chromatograph (GC), and a Clarus 600S mass spectrometer (MS) with flame ionization detector (FID) was used at a pyrolysis temperature of 500°C (20°C·ms$^{-1}$, heating rate; 30 s, hold time). The compounds were immediately trapped in a cold Tenax®-TA adsorbent trap (to avoid any additional secondary reactions). The trap was heated up to 350°C with the pyrolysis products then transferred to the GC column via a heated transfer line (300°C) using an inert Helium carrier gas (20 mL·min$^{-1}$). The pyrolysis products were separated using a 30 m Elite-1701 (PerkinElmer, Llantrisant, UK) capillary separation column maintained at a temperature of 350°C, with the GC injection port kept at a temperature of 275°C with a 1:125 split ratio. The FID detector was held at 275°C with a hydrogen–air combustion mixture (with constant flows of 45 mL·min$^{-1}$ and 450 mL·min$^{-1}$ for hydrogen and air, respectively). The chromatogram analysis was performed using OpenChrom in conjunction with the NIST11 mass spectra library to identify compounds in the pyrolysis vapours using a match factor of 70% or higher. The tubes were calcined after the reaction in a Carbolite furnace at 700°C for 15 min to determine the solid products of the reaction. The solid product yield was calculated by dividing the remaining mass (char) by the initial weight of PHA extract. Samples were

analysed in duplicate. The pyrolysis product (char, crotonic acid, and other vapours) yields were calculated as follows:

$$Yield_{char}\ (\%) = (m_f/m_i) \times 100 \qquad \text{Eq. 5}$$

Where,

$m_f$ is the final total mass (char)

$m_i$ is the initial total mass

$$Yield_{crotonic\ acid}\ (\%) = [((m_i - m_f) \times F_c)/m_i\,] \times 100 \qquad \text{Eq. 6}$$

Where,

$F_c$ is the fraction of crotonic acid in the pyrolysis products

$$Yield_{other\ vapours}\ (\%) = [((m_i - m_f) \times (1 - F_c))/m_i\ ] \times 100 \qquad \text{Eq. 7}$$

## RESULTS AND DISCUSSION

Analysis of the microbial biomass waste (MBW) obtained upon magnetosome purification

In our recent work, we have developed a simple pH-stat fermentation strategy that affords growth of *Mgryph* to relatively high cell densities. There, cellular PHA content was shown to be inversely correlated to magnetosome production, showing a remarkably high accumulation at a late phase of the culture [26]. In this work, the magnetosome production corresponded to 10.1 ± 1.2 mg iron·g$^{-1}$ DCW whereas the purified extract of magnetosomes contained 1.4 mg iron·mL$^{-1}$. In order to rapidly evaluate the presence of PHA in the "wash" fractions generated upon the magnetosome purification, the fluorometric methodology described in the M&M section was applied. Each of the nine "wash" fractions were evaluated for PHA content using Pyr-546, a fluorophore that binds lipid-like molecules such as PHA which has been reported to bind *Mgryph* PHA [23] successfully. Figure 1 shows the results of the Pyr-546-stained PHA using fluorometric assay and fluorescence microscopy of each of the "wash" fractions (n=1). As can be observed, relative fluorescence values in wash 1 are low, which is due to the detector's

saturation due to the high concentration of biomass in the sample. Therefore, relative PHA content determined from the fluorometry assay was underestimated in "Wash 1" fraction, as evidenced by the image obtained for the very same sample using fluorescence microscopy showing large amounts of PHAs aggregates. Results from "wash" fractions 2 – 4 indicate a rapid decrease of PHA content, whereas "wash" fractions 5 – 9 do not show a significant decrease of PHA content. This assay will help in future studies to identify the fractions with the highest PHA content to be used for further processing. The nine fractions were subsequently combined (180 mL) to recover PHA, and thus obtaining the microbial waste biomass (MBW) used for subsequent analysis and treatment.

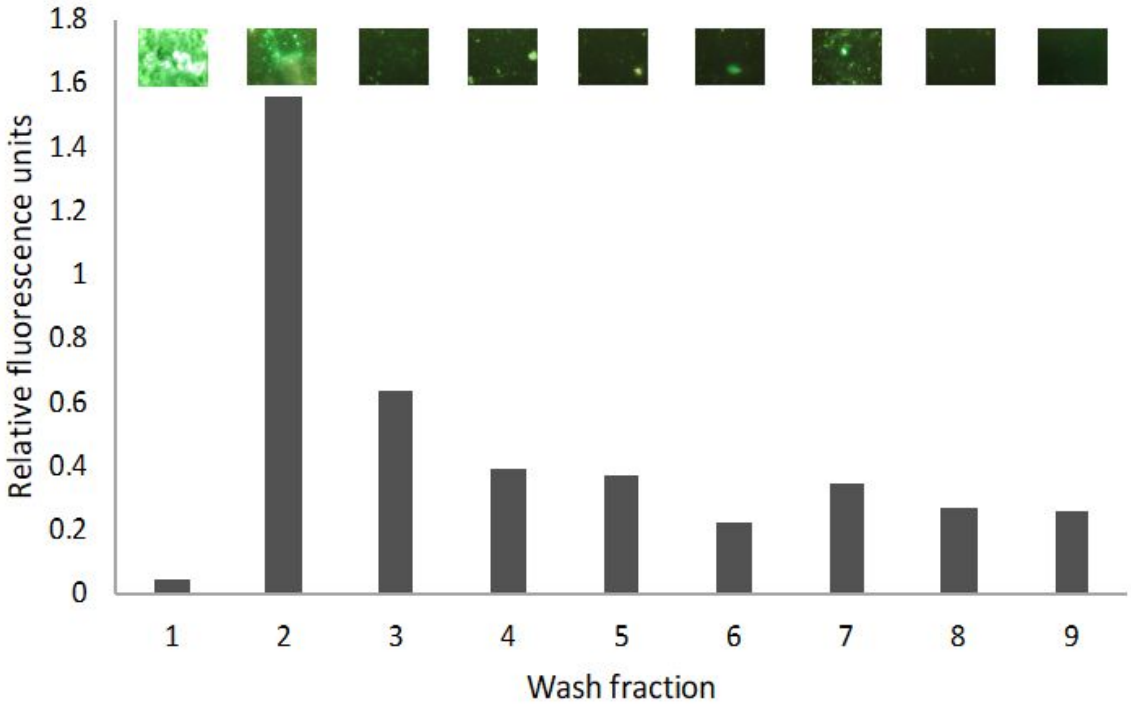


**Figure 1.** Relative fluorescence (graph) and fluorescence microscopy (top images) of the nine wash fractions obtained through the purification of magnetosomes from *Magnetospirillum gryphiswaldense* (*Mgryph*). Green fluorescence corresponds to Pyr-546-stained PHA granules.

Recovery of polyhydroxyalkanoates (PHA) from *Mgryph* MBW

The quantification of PHA in intact cells (*Mgryph* homogenised) was determined to be 17.5% of the total dry cell weight. The MBW generated after cell disruption, and magnetosome extraction was used to recover PHA from *Mgryph*. Following freeze-drying of the MBW, three concentration levels (10, 30 or 50 g MBW·$L^{-1}$ NaClO (13% (w/v)) were prepared, and extraction of PHA was evaluated.

GC-MS analysis revealed the presence of 3-hydroxybutyric acid (3HB) copolymerized with 3-hydroxyvaleric acid (3HV), as can be observed in the chromatograms shown in Figure 2. For example, the GC-MS chromatogram is shown in Figure 2C for the PHA extracted from *Mgryph* (10 g MBW·$L^{-1}$) using NaClO (13% (w/v)). The chromatograms for the PHA extracted from *Mgryph* (30 and 50 g MBW·$L^{-1}$) using NaClO (13% (w/v)) are available in the supplementary materials (Figure S1). The calculated relative abundance of 3HB:3HV was 99:1 (mol%). This relative abundance is similar to values obtained in different microbial systems such as *C. necator* where 3HB:3HV (98.5:1.5) was achieved when growing bacteria on Rapeseed meal hydrolysate supplemented with mineral medium [43]. To the best of our knowledge, this is the first time where the production of poly(3-hydroxybutyrate-co-3-hydroxyvalerate) is described in *Mgryph*.

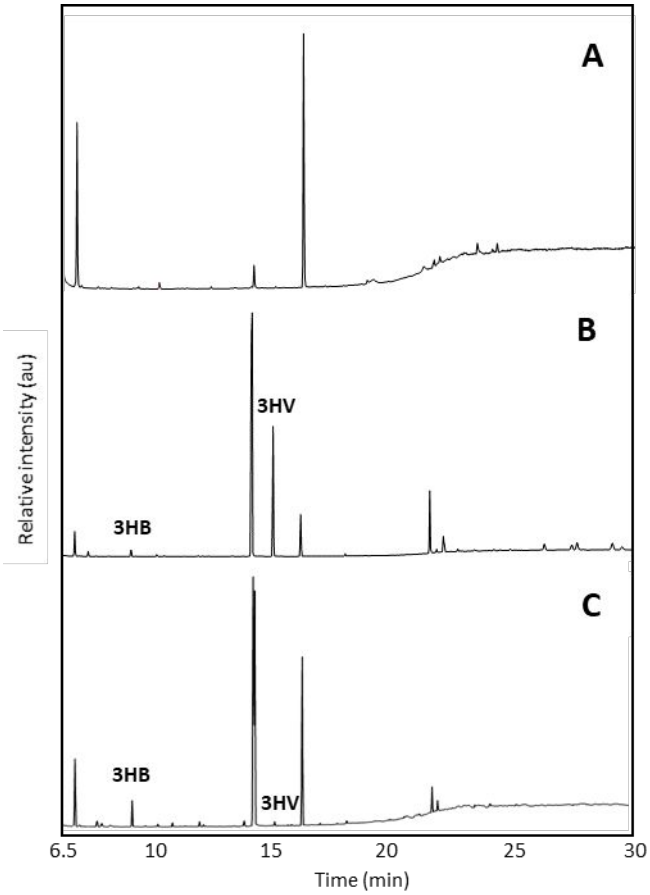


**Figure 2.** Total ion current (TIC) GC-MS chromatograms of (A) blank sample, (B) standard P(3HB-co-3HV) copolymer with a 3HV content of 8 mol% and (C) PHA extracted from *Mgryph* (10 g MBW·L$^{-1}$) using NaClO (13% (w/v)). 3HB: 3-hydroxybutyric acid; 3HV: 3-hydroxyvaleric acid.

As shown in Table 1, the maximum recovery of PHA was achieved for the 10 g MBW·L$^{-1}$. The content of PHA in the cells (*Mgryph* homogenised) and the MBW were 17.5% and 5.1%, respectively. The difference in PHA content between these fractions can be explained by (i) the dilution effect due to differences in the volume of each fraction – 25 mL for *Mgryph* cells in the homogenised *vs.* 180 mL for the MBW, and (ii) the loss of PHA during the magnetosome purification process, whereby the calculated PHA yield after cell disruption and after pulling all the wash fractions to make up the MBW, was 92.3%, meaning that 7.7% of PHA was lost. Both measurements in this experiment were carried out once to avoid losing significant volume

of sample. These observations are consistent with PHB content measurements carried out in our lab in similar experimental conditions (not published).

The GC-MS analysis of the extracts after NaClO treatment indicated that up to 51.3% of the content corresponded to PHA. This value is relatively low compared to results obtained elsewhere for other PHA-accumulating microorganisms such as *Bacillus axaraqunsis* [44] and *Bulkhoderia cepacia* B27 [45] after NaClO extraction. However, our results may likely be underestimating the total PHA concentration due to the limitation of the GC-MS analysis: other lipid-like molecules or proteins that are associated with the extracted PHA cannot be detected [46]. *Mgryph* was grown in this study using lactic acid as the sole carbon source. It has been widely acknowledged that some PHA-accumulating bacteria are capable of producing different types of homo and hetero-polymers (i.e. PHB [poly(3-hydroxybutyric acid)], and/or P(3HB-co-3HV) [poly(3-hydroxybutyric-co-3-hydroxyvaleric acid)] when organic acids are added as the carbon source [47–49]. The overall and extraction yields are presented in Table 1. The optimal overall and extraction yields were found for the 10 g MBW·L$^{-1}$ condition, 90.3% and 97.8%, respectively. These results confirm the suitability of using NaClO as an efficient and cost-effective extraction methodology of PHA. The experiments performed using 30 g MBW·L$^{-1}$ and 50 g MBW·L$^{-1}$ presented similar values, indicating that an excess of biomass concentration might saturate the system and, therefore, PHA are not extracted efficiently.

**Table 1.** Recovery of PHA using sodium hypochlorite (NaClO) extraction

| Step | PHA % (mg PHA/100 mg DW) | Total PHA (mg) | Overall Yield (%) | Extraction Yield (%) | Purification factor |
|---|---|---|---|---|---|
| *Mgryph* homogenised | 17.5 | 9.17 | 100.0 | - | 1 |
| MBW | 5.1 | 8.47 | 92.3 | 100.0 | 0.29 |
| NaClO extraction (10 g MBW/L) | 51.3 ± 0.14[a] | 8.28 | 90.3 | 97.8 | 2.93 |
| NaClO extraction (30 g MBW/L) | 35.0 ± 1.3[a] | 6.67 | 72.8 | 78.8 | 2.01 |
| NaClO extraction (50 g MBW/L) | 26.9 ± 0.53[a] | 6.88 | 75.0 | 81.2 | 1.54 |

[a]Mean and standard deviation values from three independent extraction experiments. [b]Mean and standard deviation values of nine untreated samples. MBW: Microbial biomass waste

Thermogravimetric analysis of PHA

The evaluation of PHA extracted from *Mgryph* was carried out by thermogravimetric analysis (TGA). The thermal degradation is almost exclusively a mechanism involving a random chain scission of the polymer with a cis-elimination reaction involving a six-membered ring transition state [50]. Our results revealed an inverse correlation between purity and concentration of MBW used for PHA extraction with NaClO. As can be seen in the representative thermograms (n=2) in Figure 3, PHA purities of 73 ± 2%, 63 ± 2%, 60 ± 2% and 16 ± 1% were calculated for samples prepared with 10, 30, and 50 g MBW·$L^{-1}$ and, untreated; respectively (Figure 3A). Our optimal PHA purity values are higher when compared to extraction of PHA from *Bacillus axaraqunsis* [44] and *Bulkhoderia cepacia* B27 [45] using NaClO. Comparable purity values obtained under similar experimental conditions have been previously reported [51]. However, our PHA purity values are slightly lower than other works that have systematically optimised PHA extraction by evaluating the effect of NaClO concentration and incubation temperature [52] and have also assessed the effect of different surfactants [51]. Nonetheless, and to the best of our knowledge, our study is the first to extract PHA from *Mgryph*, thus representing a benchmark for future optimization studies for PHA recovery in this microorganism. Our TGA results indicate a PHA purity of 73 ± 4%. In contrast, GC-MS analysis revealed a PHB content of 51.3 ± 0.14%. This difference of c.a. 21.7% is likely due to the presence of PHA, whose

monomer structure has not been resolved in this study. Subsequently, further investigations will be needed to fully characterise *Mgryph* PHA using, for example, differential scanning calorimetry (DSC) to determine the composition or thin-layer chromatography to determine the polymer molecular weight. The thermogravimetric analysis of PHA extracts from *Mgryph* showed a degradation range between 232 – 292°C (Figure 3B). The peak degradation temperature of PHA extracted from *Mgryph* was identified to be 276°C, 254°C and 260°C for the 10, 30 or 50 g MBW·$L^{-1}$, respectively. The peak degradation temperature of the untreated MBW was identified to be 248°C. These results are comparable to literature about different monomer compositions of the PHBV [53–55]. In contrast, the peak degradation of commercial 3-hydroxybutyric acid (3HB) with a purity of 92% (95% according to the manufacturer) was identified at 316°C. This difference in the degradation temperature may be attributed to sample purity and structural variations: the homopolymer of PHB has been previously determined to have a higher degradation temperature when compared to polyhydroxyalkanoates P(3HA) and co-polymers P(3HB-co-3HV) [56].

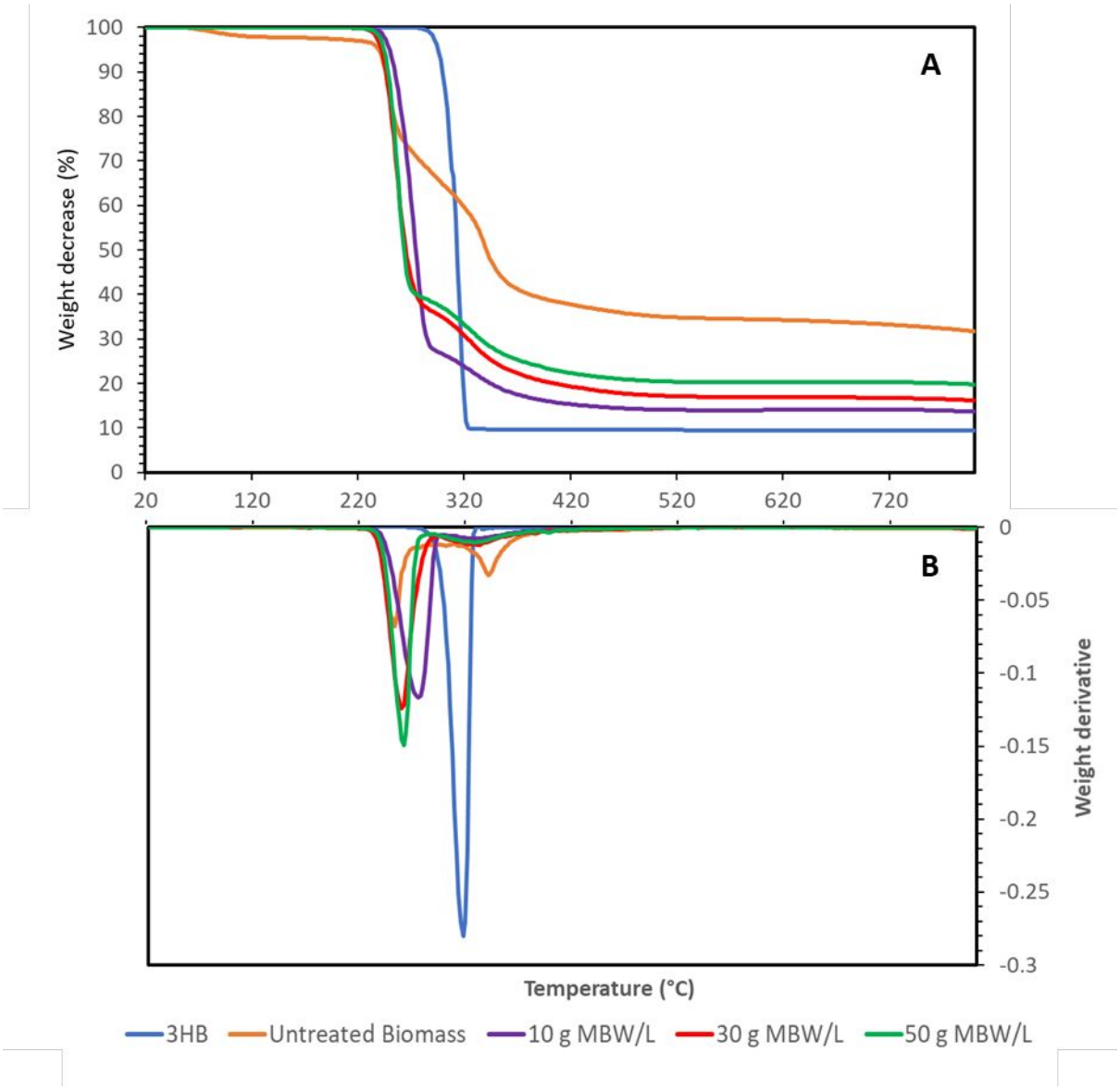


**Figure 3.** Thermogravimetric analysis of PHA produced by *Magnetospirillum gryphiswaldense* (*Mgryph*). (A) Weight decrease and (B) weight derivative profiles of 3HB (3-hydroxybutyric acid); untreated microbial biomass waste (MBW); and NaClO-treated samples (10, 30, 50 MBW/L)

Protein content in the aqueous fraction using NaClO extraction

We quantified protein concentration to examine the potential for upgrading the aqueous fraction obtained from the NaClO extraction. First, the intracellular protein concentration in *Mgryph* cells was determined as 146.8 mg·g$^{-1}$ DCW, corresponding to 5.5 mg·mL$^{-1}$ in the

homogenized (32% WCW·L$^{-1}$) (Table 2) before the sonication step. After the MBW was collected and prepared as described in the M&M section, there was a significant loss of 39.6% protein. This might be due to their degradation and the protein fraction as part of the purified magnetosomes (not measured). We observed that the protein extraction yield was inversely correlated to the MBW concentration employed for the NaClO extraction step and this is likely to occur due to the presence of undigested MBW that is found in the sediment (at 30 and 50 g MBW·L$^{-1}$) containing protein among other cellular components. Our results agree with previous work that showed that optimal biomass digestion occurs at concentrations lower than 30 g·L$^{-1}$ under experimental conditions similar to those in our study [40]. Despite the non-optimised recovery, more than half of the cellular protein can potentially be further processed and upgraded, then used as an additive in animal feed or agriculture, thanks to its rich C/N composition [7,8].

**Table 2.** Recovery of total soluble protein after PHA extraction from *Mgryph*

| Step | Protein concentration (mg/mL)[a] | Total Protein (mg) | Overall Yield (%) | Extraction Yield (%) |
|---|---|---|---|---|
| *Mgryph* homogenised | 5.55 ± 0.11 | 138.8 (7.71)[b] | 100.0 | - |
| MBW[c] | 0.233 ± 0.008 | 4.66 | 60.4 | 100.0 |
| NaClO extraction (10 g MBW/L) | 0.152 ± 0.002 | 4.11 | 53.3 | 88.1 |
| NaClO extraction (30 g MBW/L) | 0.156 ± 0.008 | 1.14 | 14.7 | 24.4 |
| NaClO extraction (50 g MBW/L) | 0.150 ± 0.002 | 0.87 | 11.3 | 18.7 |

[a]Mean and standard deviation values of duplicated measurements. [b]Amount of protein used for subsequent steps.[c]Microbial biomass waste lyophilised and untreated.

Pyrolysis of PHB, untreated Microbial waste biomass, and Mgryph PHA extracts

Pyrolysis of *Mgryph* PHA extracts was carried out to evaluate the potential to obtain added value biochemicals. Isothermal pyrolysis tests were conducted as per the method described in section 2.6. The pyrolysis temperature was set to 300°C as previous studies on PHB pyrolysis

found this value to be optimal to ensure vaporisation of PHB [36]. Our TGA analysis results confirmed that PHA extracts from *Mgryph* are vaporised at temperatures lower than 300°C (Figure 3). The total ion current (TIC) chromatograms of the pyrolyzed products are shown in Figure 4. Pyrolysis products from untreated MBW (Figure 4A) showed a group of peaks at retention times t = 11.07 min, t = 11.83 min and t = 15.32 min with the characteristic signals at *m/z* = 39, 41, 68 and 86 that could be assigned to crotonic acid isomers. A few other peaks also appear at different retention times (2.31, 4.60, 9.60, 18.41 and 20.81 min). However, the product compounds were not reliably assigned to molecules in the library, which may correspond to sample impurities. Pyrograms obtained for the three different NaClO treatment conditions (10, 30 and 50 g MBW·$L^{-1}$) presented a similar profile. As an example, a pyrogram of PHA extracts obtained using 10 g MBW·$L^{-1}$ using NaClO (13% w/v)) is presented (Figure 4B). As observed, peaks 1 & 2 corresponding to crotonic acid were observed in PHA extracted from MBW using NaClO. In addition, the group of peaks 4, 5 & 6 (Figure 4B) revealed the characteristic signals *m/z* = 41, 68, 69, 86 and 103 that could be assigned to dimers or trimers of crotonic acid in accordance with previously published works [50,57]. Only the PHA extracts obtained using 50 g MBW·$L^{-1}$ (Figure S2) presented two additional peaks at a retention time of t = 2.27 and t = 9.91, which were also observed in untreated MBW samples (Figure 4A). These peaks were not accurately assigned, and these might correspond to by-products from sample impurities. Pyrolysis products from standard 3-hydroxybutyric acid (Figure 4C) show a peak at a retention time t = 11.91 min corresponding to crotonic acid (peak 1). A larger peak at a retention time t = 17.62 (peak 2) min was observed corresponding to iso-crotonic acid based on its characteristic signal at *m/z* = 41, 68, and 86. Although iso-crotonic acid has a similar molecular formula to crotonic acid, differences in geometric orientation cause a variation in boiling points, and therefore different retention time [58]. The standard compound

analysis confirmed the presence of crotonic acid in both the untreated MBW and extracted PHA.

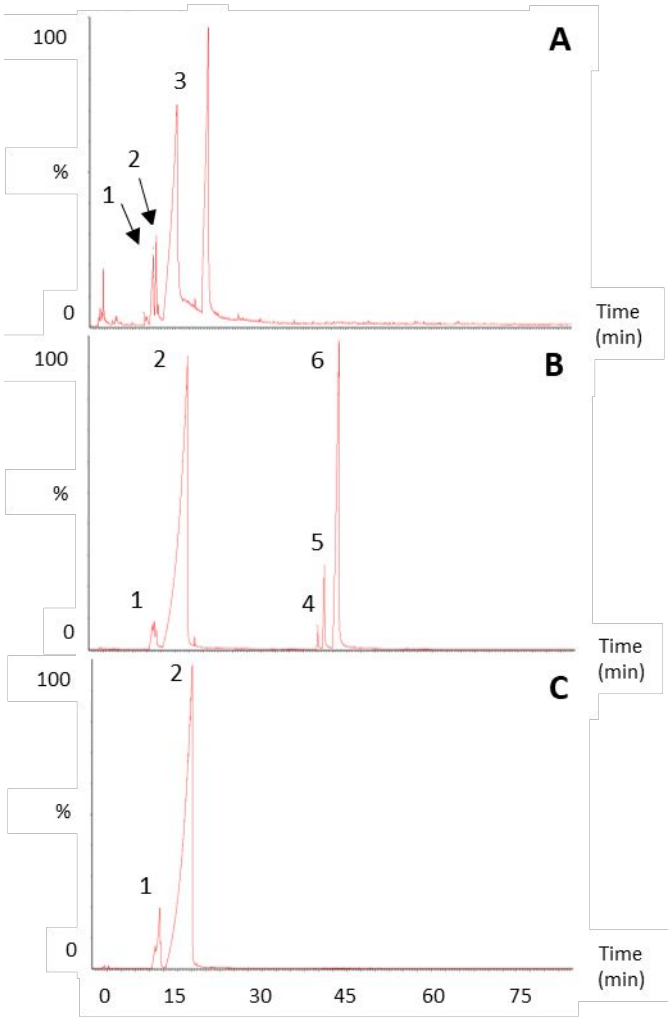


**Figure 4.** Total ion current (TIC) pyrograms of (A) untreated microbial waste biomass (MBW), (B) PHA extracted from *Mgryph* (10 g MBW·L$^{-1}$) using NaClO (13% (w/v)) and (C) standard 3-hydroxybutyric acid (3HB, 95% purity). 1, 2 & 3: Isomers of crotonic acid monomers; 4, 5 & 6: Isomers of crotonic acid dimers.

The pyrolysis product yields were calculated using equations 4 – 6 (please refer to the M&M section) to evaluate the MBW concentration-effect before NaClO extraction. The amount of char corresponded to the remaining sample quantity after pyrolysis, whereas the vaporised

fraction corresponds to crotonic acid and the "other" vapours. From Figure 5, it is evident that commercial 3-hydroxybutyric acid (3HB) mostly yields crotonic acid (96.6 wt.%) and a low fraction of char (3.4 wt.%). The pyrolysis of the untreated MBW resulted in increased char content (54 wt.%) when compared to the other samples and a significant fraction of un-assigned vapour compounds (20.6 wt.%), likely due to the impurities present in the sample. The analysis of NaClO-treated samples revealed that the fraction corresponding to char was between 13.0% and 17.2% without a clear trend. For the NaClO-treated sample, the higher crotonic acid yield of 86 wt.% was obtained for the condition using 10 g MBW·L$^{-1}$, whereas the conditions using 30 g MBW·L$^{-1}$ and 50 g MBW·L$^{-1}$ revealed similar crotonic acid yields around 80 wt.%. The char yield of PHA extracts (post-NaClO treatment) was proportional to the initial concentration of MBW, which is likely due to the increase of impurities in the samples.

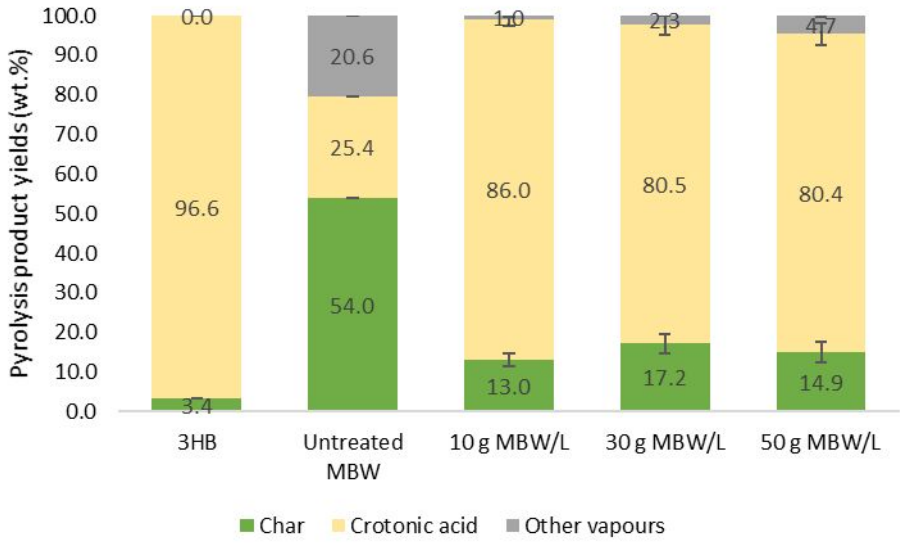


**Figure 5.** Pyrolysis products yields distribution for 3HB (3-hydroxybutyric acid); untreated microbial biomass waste (MBW); and NaClO-treated samples (10, 30, 50 MBW/L).

Several studies have reported the pyrolysis of microbial biopolymers such as PHB as an upgrading step, where crotonic acid and oligomers containing crotonated groups are the dominant end products. For example, Grassie and Murray quantified crotonic acid production

during the pyrolysis of PHB at 500°C resulting in c.a. 40% yield [59]. Vu and co-workers obtained crotonic acid with yields of 60–65% and 20–25% from purified and dried bacterial cells, respectively [60]. The cost-effective production of PHA has been proposed using wastewater treatment [61] or as an added-value product from anaerobic digestion (AD) [62]. Recent works have developed $H_2$ and PHB co-production processes under dark fermentation, photo fermentation, and subsequent dark-photo fermentation [63]. Moreover, other studies have developed integrated algae-based biorefineries for the co-production of biodiesel, astaxanthin and PHB [64]. These two examples demonstrate the growing interest in developing more sustainable, cost-effective and clean processes through integrated co-production technologies. In contrast, the accumulation of PHA in *Mgryph* has been considered before this work as a competing element in the process of magnetosome production [34] rather than an opportunity to co-produce two bio-based products simultaneously. Here, we envisaged the development of MTB-based biorefineries for the co-production of magnetosomes, PHA, and proteins, including a further upgrade of PHA into crotonic acid (Figure 6). The latter has seen an increase in its market potential as a bio-based alternative to petrochemicals which can be used as a precursor for several important chemicals such as maleic anhydride, acrylic acid, butanol and propylene [36].

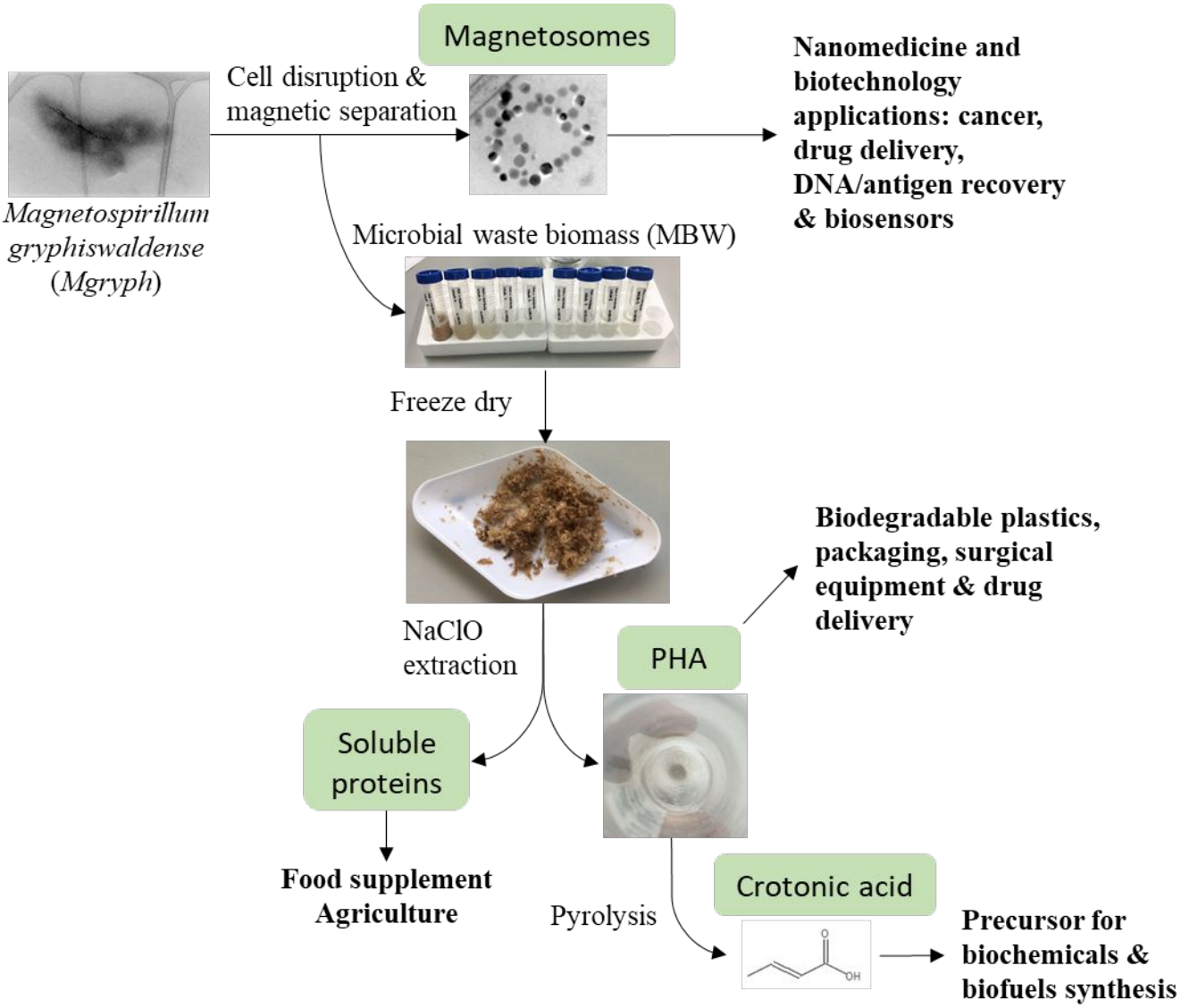


**Figure 6.** Diagram of the Magnetotactic bacteria-based biorefinery concept for the co-production of magnetosomes, proteins, polyhydroxyalkanoates (PHA) and crotonic acid.

## CONCLUSIONS

This work represents a novel contribution towards the development of magnetotactic bacteria-based biorefineries that have the potential to have a positive impact on the efficiency and economy of the magnetosome production process, including the utilisation of microbial biomass waste (MBW) thus, improving the environmental performance of magnetosome

production whilst co-producing chemicals with added value through green technologies. To the best of our knowledge, our study is the first to extract PHA from *Mgryph*, thus representing a benchmark for future optimization studies for PHA recovery in this microorganism. In order to ensure industrial deployment of this technology, fully scalable process units will be required as well as techno-economic studies to evaluate its engineering and economic feasibility.

## ACKNOWLEDGMENTS

The work was supported by the Royal Society Research Grant RGS\R1\191377; the Aston Institute of Materials Research (AIMR) Seed-corn grant; the Energy Research Accelerator (ERA) grant from Innovate UK. Carmen Hierro-Iglesias acknowledges Aston University for an EAS-funded PhD studentship. Marta Masó-Martínez acknowledges Aston University for an EPSRC-DTP-funded PhD studentship. The authors acknowledge the assistance of Gurpreet Jaswal in the *Mgryph* growth experiments. The authors acknowledge Dr Stylianos Stefanidis for assistance with the pyrolysis experiments.

## CONFLICTS OF INTEREST

The authors declare no competing financial interest.

## ASSOCIATED CONTENT

### Supporting information

The following Supporting Information is available free of charge at the ACS website:

**Figure S1.** Total ion current (TIC) GC-MS chromatograms of PHA extracted from *Mgryph* using NaClO (13% (w/v)) containing (A) 30 g MBW·$L^{-1}$ and (B) 50 g MBW·$L^{-1}$. 3HB: 3-hydroxybutyric acid; 3HV: 3-hydroxyvaleric acid.

**Figure S2.** Total ion current (TIC) pyrograms of PHA extracted from *Mgryph* using NaClO (13% (w/v)) and microbial biomass waste concentration (MBW) of (A) 30 g·$L^{-1}$ and (B) 50 g·$L^{-1}$.

AUTHOR INFORMATION

**Corresponding Author**

Alfred Fernández-Castané – Energy and Bioproducts Research Institute & Aston Institute of Materials Research, Aston University, Birmingham, B4 7ET, UK; Email: a.fernandez-castane1@aston.ac.uk

**REFERENCES**

(1) M'barek, R.; Philippidis, G.; Ronzon, T. *Alternative Global Transition Pathways to 2050: Prospects for the Bioeconomy: An Application of the MAGNET Model with SDG Insights*; **2019**. https://doi.org/10.2760/594847.

(2) Mata, T. M.; Martins, A. A.; Caetano, N. S. Microalgae for Biodiesel Production and Other Applications: A Review. *Renew. Sustain. Energy Rev.* **2010**, *14* (1), 217–232. https://doi.org/10.1016/j.rser.2009.07.020.

(3) Kumar, A.; Saini, H. S.; Kumar, S. Bioleaching of Gold and Silver from Waste Printed Circuit Boards by Pseudomonas Balearica SAE1 Isolated from an E-Waste Recycling

Facility. *Curr. Microbiol.* **2018**, *75* (2), 194–201. https://doi.org/10.1007/s00284-017-1365-0.

(4) Wang, B.; Ma, J.; Zhang, L.; Su, Y.; Xie, Y.; Ahmad, Z.; Xie, B. The Synergistic Strategy and Microbial Ecology of the Anaerobic Co-Digestion of Food Waste under the Regulation of Domestic Garbage Classification in China. *Sci. Total Environ.* **2021**, *765*, 144632. https://doi.org/10.1016/j.scitotenv.2020.144632.

(5) Ruiz, J.; Fernández-Castané, A.; de Mas, C.; González, G.; López-Santín, J. From Laboratory to Pilot Plant E. Coli Fed-Batch Cultures: Optimizing the Cellular Environment for Protein Maximization. *J Ind Microbiol Biotechnol* **2013**, *40* (3), 335–343. https://doi.org/10.1007/s10295-012-1226-6.

(6) Hara, K. Y.; Araki, M.; Okai, N.; Wakai, S.; Hasunuma, T.; Kondo, A. Development of Bio-Based Fine Chemical Production through Synthetic Bioengineering. *Microb. Cell Fact.* **2014**, *13* (1). https://doi.org/10.1186/s12934-014-0173-5.

(7) Sullivan, C. T.; Harman, R. M.; Eash, N. S.; Zahn, J. A.; Goddard, J. J.; Walker, F. R.; Saxton, A. M.; Lambert, D. M.; McIntosh, D. W.; Hart, W. E.; Freeland, R. S.; Morrison, J. E. Utilization of Spent Microbial Biomass as an Alternative Crop Nitrogen Source. *Agron. J.* **2017**, *109* (5), 1870–1879. https://doi.org/10.2134/agronj2016.12.0742.

(8) Shurson, G.; Spiehs, M.; Whitney, M. The Use of Maize Distiller's Dried Grains with Solubles in Pig Diets. *Anim. Rev. Pig News Inf.* **2004**, *25* (92), 75–83.

(9) Bazylinski, D. A.; Frankel, R. B. Magnetosome Formation in Prokaryotes. *Nature Reviews Microbiology*. Nature Publishing Group March 2004, pp 217–230. https://doi.org/10.1038/nrmicro842.

(10) Borg, S.; Rothenstein, D.; Bill, J.; Schüler, D. Generation of Multishell Magnetic Hybrid Nanoparticles by Encapsulation of Genetically Engineered and Fluorescent

Bacterial Magnetosomes with ZnO and $SiO_2$. *Small* **2015**, *11* (33), 4209–4217. https://doi.org/10.1002/smll.201500028.

(11) Le Fèvre, R.; Durand-Dubief, M.; Chebbi, I.; Mandawala, C.; Lagroix, F.; Valet, J. P.; Idbaih, A.; Adam, C.; Delattre, J. Y.; Schmitt, C.; Maake, C.; Guyot, F.; Alphandéry, E. Enhanced Antitumor Efficacy of Biocompatible Magnetosomes for the Magnetic Hyperthermia Treatment of Glioblastoma. *Theranostics* **2017**, *7* (18), 4618–4631. https://doi.org/10.7150/thno.18927.

(12) Mannucci, S.; Ghin, L.; Conti, G.; Tambalo, S.; Lascialfari, A.; Orlando, T.; Benati, D.; Bernardi, P.; Betterle, N.; Bassi, R.; Marzola, P.; Sbarbati, A. Magnetic Nanoparticles from Magnetospirillum Gryphiswaldense Increase the Efficacy of Thermotherapy in a Model of Colon Carcinoma. *PLoS One* **2014**, *9* (10). https://doi.org/10.1371/journal.pone.0108959.

(13) Zhang, Y.; Ni, Q.; Xu, C.; Wan, B.; Geng, Y.; Zheng, G.; Yang, Z.; Tao, J.; Zhao, Y.; Wen, J.; Zhang, J.; Wang, S.; Tang, Y.; Li, Y.; Zhang, Q.; Liu, L.; Teng, Z.; Lu, G. Smart Bacterial Magnetic Nanoparticles for Tumor-Targeting Magnetic Resonance Imaging of HER2-Positive Breast Cancers. *ACS Appl. Mater. Interfaces* **2019**, *11* (4), 3654–3665. https://doi.org/10.1021/acsami.8b15838.

(14) Boucher, M.; Geffroy, F.; Prévéral, S.; Bellanger, L.; Selingue, E.; Adryanczyk-Perrier, G.; Péan, M.; Lefèvre, C. T.; Pignol, D.; Ginet, N.; Mériaux, S. Genetically Tailored Magnetosomes Used as MRI Probe for Molecular Imaging of Brain Tumor. *Biomaterials* **2017**, *121*, 167–178. https://doi.org/10.1016/j.biomaterials.2016.12.013.

(15) Revathy, T.; Jacob, J. J.; Jayasri, M. A.; Suthindhiran, K. Microbial Biofilm Prevention on Wound Dressing by Nanobiocoating Using Magnetosomes-Coupled Lemon Grass Extract. *IET Nanobiotechnology* **2017**, *11* (6), 738–745. https://doi.org/10.1049/iet-nbt.2016.0236.

(16) Theerthagiri, R.; Achuthanandan, J. M.; Krishnamurthy, S. Antimicrobial Magnetosomes for Topical Antimicrobial Therapy. In *Nanobiomaterials in Antimicrobial Therapy: Applications of Nanobiomaterials*; Elsevier Inc., **2016**; pp 67–101. https://doi.org/10.1016/B978-0-323-42864-4.00003-8.

(17) Smit, B. A.; Van Zyl, E.; Joubert, J. J.; Meyer, W.; Prévéral, S.; Lefèvre, C. T.; Venter, S. N. Magnetotactic Bacteria Used to Generate Electricity Based on Faraday's Law of Electromagnetic Induction. *Lett. Appl. Microbiol.* **2018**, *66* (5), 362–367. https://doi.org/10.1111/lam.12862.

(18) Tanaka, M.; Knowles, W.; Brown, R.; Hondow, N.; Arakaki, A.; Baldwin, S.; Staniland, S.; Matsunaga, T. Biomagnetic Recovery and Bioaccumulation of Selenium Granules in Magnetotactic Bacteria. *Appl. Environ. Microbiol.* **2016**, *82* (13), 3886–3891. https://doi.org/10.1128/AEM.00508-16.

(19) Ali, I.; Peng, C.; Khan, Z. M.; Naz, I.; Sultan, M. An Overview of Heavy Metal Removal from Wastewater Using Magnetotactic Bacteria. *J. Chem. Technol. Biotechnol.* **2018**, *93* (10), 2817–2832. https://doi.org/10.1002/jctb.5648.

(20) Sannigrahi, S.; Suthindhiran, K. Metal Recovery from Printed Circuit Boards by Magnetotactic Bacteria. *Hydrometallurgy* **2019**, *187* (April), 113–124. https://doi.org/10.1016/j.hydromet.2019.05.007.

(21) Lohße, A.; Ullrich, S.; Katzmann, E.; Borg, S.; Wanner, G.; Richter, M.; Voigt, B.; Schweder, T.; Schüler, D. Functional Analysis of the Magnetosome Island in Magnetospirillum Gryphiswaldense: The MamAB Operon Is Sufficient for Magnetite Biomineralization. *PLoS One* **2011**, *6* (10). https://doi.org/10.1371/journal.pone.0025561.

(22) Uebe, R.; Schüler, D. Magnetosome Biogenesis in Magnetotactic Bacteria. *Nat. Rev. Microbiol.* **2016**, *14* (10), 621–637. https://doi.org/10.1038/nrmicro.2016.99.

(23) Fernández-Castané, A.; Li, H.; Thomas, O. R.; Overton, T. W. Flow Cytometry as a Rapid Analytical Tool to Determine Physiological Responses to Changing O2 and Iron Concentration by Magnetospirillum Gryphiswaldense Strain MSR-1. *Sci. Rep.* **2017**, 7:13118.

(24) Schultheiss, D.; Schüler, D. Development of a Genetic System for Magnetospirillum Gryphiswaldense. *Arch. Microbiol.* **2003**, *179* (2), 89–94. https://doi.org/10.1007/s00203-002-0498-z.

(25) Zhang, Y.; Zhang, X.; Jiang, W.; Li, Y.; Li, J. Semicontinuous Culture of Magnetospirillum Gryphiswaldense MSR-1 Cells in an Autofermentor by Nutrient-Balanced and Isosmotic Feeding Strategies. *Appl. Environ. Microbiol.* **2011**, *77* (17), 5851–5856. https://doi.org/10.1128/AEM.05962-11.

(26) Fernández-Castané, A.; Li, H.; Thomas, O. R. T.; Overton, T. W. Development of a Simple Intensified Fermentation Strategy for Growth of Magnetospirillum Gryphiswaldense MSR-1: Physiological Responses to Changing Environmental Conditions. *N. Biotechnol.* **2018**, *46* (June), 22–30. https://doi.org/10.1016/j.nbt.2018.05.1201.

(27) Berny, C.; Le Fèvre, R.; Guyot, F.; Blondeau, K.; Guizonne, C.; Rousseau, E.; Bayan, N.; Alphandéry, E. A Method for Producing Highly Pure Magnetosomes in Large Quantity for Medical Applications Using Magnetospirillum Gryphiswaldense MSR-1 Magnetotactic Bacteria Amplified in Minimal Growth Media. *Front. Bioeng. Biotechnol.* **2020**, *8*. https://doi.org/10.3389/fbioe.2020.00016.

(28) Grünberg, K.; Müller, E. C.; Otto, A.; Reszka, R.; Linder, D.; Kube, M.; Reinhardt, R.; Schüler, D. Biochemical and Proteomic Analysis of the Magnetosome Membrane in Magnetospirillum Gryphiswaldense. *Appl. Environ. Microbiol.* **2004**, *70* (2), 1040–1050. https://doi.org/10.1128/AEM.70.2.1040-1050.2004.

(29) Lohße, A.; Kolinko, I.; Raschdorf, O.; Uebe, R.; Borg, S.; Brachmann, A.; Plitzko, J. M.; Müller, R.; Zhang, Y.; Schüler, D. Overproduction of Magnetosomes by Genomic Amplification of Biosynthesis-Related Gene Clusters in a Magnetotactic Bacterium. *Appl. Environ. Microbiol.* **2016**, *82* (10), 3032–3041. https://doi.org/10.1128/AEM.03860-15.

(30) Fernández-Castané, A.; Li, H.; Joseph, S.; Ebeler, M.; Franzreb, M.; Bracewell, D. G.; Overton, T. W.; Thomas, O. R. T. Nanoparticle Tracking Analysis: A Robust Tool for Characterizing Magnetosomes Preparations. *Food Bioprod. Process.* **2021**, *127, 426-434*.

(31) Alphandéry, E.; Guyot, F.; Chebbi, I. Preparation of Chains of Magnetosomes, Isolated from Magnetospirillum Magneticum Strain AMB-1 Magnetotactic Bacteria, Yielding Efficient Treatment of Tumors Using Magnetic Hyperthermia. *Int. J. Pharm.* **2012**, *434* (1–2), 444–452. https://doi.org/10.1016/j.ijpharm.2012.06.015.

(32) Guo, F.; Liu, Y.; Chen, Y.; Tang, T.; Jiang, W.; Li, Y.; Li, J. A Novel Rapid and Continuous Procedure for Large-Scale Purification of Magnetosomes from Magnetospirillum Gryphiswaldense. *Appl. Microbiol. Biotechnol.* **2011**, *90* (4), 1277–1283. https://doi.org/10.1007/s00253-011-3189-3.

(33) Khosravi-Darani, K.; Bucci, D. Z. Application of Poly(Hydroxyalkanoate) in Food Packaging: Improvements by Nanotechnology. *Chem. Biochem. Eng. Q.* **2015**, *29* (2), 275–285. https://doi.org/10.15255/CABEQ.2014.2260.

(34) Molčan, M.; Hashim, A.; Kováč, J.; Rajňák, M.; Kopčanský, P.; Makowski, M.; Gojzewski, H.; Molokác, M.; Hvizdák, L.; Timko, M. Characterization of Magnetosomes after Exposure to the Effect of the Sonication and Ultracentrifugation. *Acta Phys. Pol. A* **2013**, *126* (1), 198–199. https://doi.org/10.12693/APhysPolA.126.198.

(35) Zhao, L.; Wu, D.; Wu, L. F.; Song, T. A Simple and Accurate Method for Quantification of Magnetosomes in Magnetotactic Bacteria by Common Spectrophotometer. *J. Biochem. Biophys. Methods* **2007**, *70* (3), 377–383. https://doi.org/10.1016/j.jbbm.2006.08.010.

(36) Mamat, M. R. Z.; Ariffin, H.; Hassan, M. A.; Mohd Zahari, M. A. K. Bio-Based Production of Crotonic Acid by Pyrolysis of Poly(3-Hydroxybutyrate) Inclusions. *J. Clean. Prod.* **2014**, *83*, 463–472. https://doi.org/10.1016/j.jclepro.2014.07.064.

(37) Blumenstein, J.; Albert, J.; Schulz, R. P.; Kohlpaintner, C. Crotonaldehyde and Crotonic Acid. In *Ullmann's Encyclopedia of Industrial Chemistry*; Wiley-VCH Verlag GmbH & Co. KGaA: Weinheim, Germany, **2015**; pp 1–20. https://doi.org/10.1002/14356007.a08_083.pub2.

(38) Mullen, C. A.; Boateng, A. A.; Schweitzer, D.; Sparks, K.; Snell, K. D. Mild Pyrolysis of P3HB/Switchgrass Blends for the Production of Bio-Oil Enriched with Crotonic Acid. *J. Anal. Appl. Pyrolysis* **2014**, *107*, 40–45. https://doi.org/10.1016/j.jaap.2014.01.022.

(39) Widdel, F.; Bak, F. Gram-Negative Mesophilic Sulfate-Reducing Bacteria. In *The prokaryotes*; Balows, A., Troper, H., Dworkin, M., Harder, W., Schleifer, K., Eds.; Springer Berlin Heidelberg: New York, **1992**; pp 3352–3378.

(40) Heinrich, D.; Madkour, M. H.; Al-Ghamdi, M. A.; Shabbaj, I. I.; Steinbüchel, A. Large Scale Extraction of Poly(3-Hydroxybutyrate) from Ralstonia Eutropha H16 Using Sodium Hypochlorite. *AMB Express* **2012**, *2* (1), 59. https://doi.org/10.1186/2191-0855-2-59.

(41) Heyen, U.; Schüler, D. Growth and Magnetosome Formation by Microaerophilic Magnetospirillum Strains in an Oxygen-Controlled Fermentor. *Appl. Microbiol. Biotechnol.* **2003**, *61* (5–6), 536–544. https://doi.org/10.1007/s00253-002-1219-x.

(42) Alves, L. P. S.; Almeida, A. T.; Cruz, L. M.; Pedrosa, F. O.; de Souza, E. M.; Chubatsu, L. S.; Müller-Santos, M.; Valdameri, G. A Simple and Efficient Method for Poly-3-Hydroxybutyrate Quantification in Diazotrophic Bacteria within 5 Minutes Using Flow Cytometry. *Brazilian J. Med. Biol. Res.* **2017**, *50* (1), 1–10. https://doi.org/10.1590/1414-431X20165492.

(43) García, I.L.; López, J.A.; Dorado, M.P. Kopsahelis, N.; Alexandri, M.; Papanikolaou, S.; Villar, M.A.; Koutinasc, A.A. Evaluation of by-products from the biodiesel industry as fermentation feedstock for poly(3-hydroxybutyrate-co-3-hydroxyvalerate) production by *Cupriavidus necator*. *Bioresour. Technol.* **2013**, 130, 16–22. https://doi.org/10.1016/j.biortech.2012.11.088

(44) Mayeli, N.; Motamedi, H.; Heidarizadeh, F. Production of Polyhydroxybutyrate by Bacillus Axaraqunsis BIPC01 Using Petrochemical Wastewater as Carbon Source. *Brazilian Arch. Biol. Technol.* **2015**, *58* (4), 643–650. https://doi.org/10.1590/S1516-8913201500048.

(45) Gamba, A. M.; Fonseca, J. S.; Méndez, D. A.; Viloria, A.; Fajardo, D.; Moreno, N. C.; Cabeza, I. O. Assessment of Different Plasticizer - Polyhydroxyalkanoate Mixtures to Obtain Biodegradable Polymeric Films. *Chem. Eng. Trans.* **2017**, *57* (June), 1363–1368. https://doi.org/10.3303/CET1757228.

(46) Pagliano, G; Galletti, P; Samorì, C.; Zaghini, A.; Torri. C. Recovery of Polyhydroxyalkanoates From Single and Mixed Microbial Cultures: A Review. *Front. Bioeng. Biotechnol.*, **2021**, 9:624021. https://doi.org/10.3389/fbioe.2021.624021

(47) Khanna, S.; Srivastava, A. K. Production of Poly(3-Hydroxybutyric-Co-3-Hydroxyvaleric Acid) Having a High Hydroxyvalerate Content with Valeric Acid Feeding. *J. Ind. Microbiol. Biotechnol.* **2007**, *34* (6), 457–461. https://doi.org/10.1007/s10295-007-0207-7.

(48) Jiang, G.; Hill, D.; Kowalczuk, M.; Johnston, B.; Adamus, G.; Irorere, V.; Radecka, I. Carbon Sources for Polyhydroxyalkanoates and an Integrated Biorefinery. *Int. J. Mol. Sci.* **2016**, *17* (7), 1157. https://doi.org/10.3390/ijms17071157.

(49) Byrom, D. Production of Poly-β-Hydroxybutyrate: Poly-β-Hydroxyvalerate Copolymers. *FEMS Microbiol. Lett.* **1992**, *103*, 247–250.

(50) Aoyagi, Y.; Yamashita, K.; Doi, Y. Thermal Degradation of Poly[(R)-3-Hydroxybutyrate], Poly[ε-Caprolactone], and Poly[(S)-Lactide]. *Polym. Degrad. Stab.* **2002**, *76* (1), 53–59. https://doi.org/10.1016/S0141-3910(01)00265-8.

(51) Mannina, G.; Presti, D.; Montiel-Jarillo, G.; Suárez-Ojeda, M. E. Bioplastic Recovery from Wastewater: A New Protocol for Polyhydroxyalkanoates (PHA) Extraction from Mixed Microbial Cultures. *Bioresour. Technol.* **2019**, *282* (March), 361–369. https://doi.org/10.1016/j.biortech.2019.03.037.

(52) Samorì, C.; Abbondanzi, F.; Galletti, P.; Giorgini, L.; Mazzocchetti, L.; Torri, C.; Tagliavini, E. Extraction of Polyhydroxyalkanoates from Mixed Microbial Cultures: Impact on Polymer Quality and Recovery. *Bioresour. Technol.* **2015**, *189*, 195–202. https://doi.org/10.1016/j.biortech.2015.03.062.

(53) Carrasco, F.; Dionisi, D.; Beccari, M.; Majone, M.; Martinelli, A. Thermal Stability of Polyhydroxyalkanotaes. *J. Appl. Polym. Sci.* **2006**, *100*, 2111–2121.

(54) Keenan, T. M.; Tanenbaum, S. W.; Stipanovic, A. J.; Nakas, J. P. Production and Characterization of Poly-β-Hydroxyalkanoate Copolymers from Burkholderia Cepacia Utilizing Xylose and Levulinic Acid. *Biotechnol. Prog.* **2004**, *20* (6), 1697–1704. https://doi.org/10.1021/bp049873d.

(55) Bengtsson, S.; Pisco, A. R.; Johansson, P.; Lemos, P. C.; Reis, M. A. M. Molecular Weight and Thermal Properties of Polyhydroxyalkanoates Produced from Fermented Sugar Molasses by Open Mixed Cultures. *J. Biotechnol.* **2010**, *147* (3–4), 172–179.

https://doi.org/10.1016/j.jbiotec.2010.03.022.

(56) Sharma, P. K.; Munir, R. I.; Blunt, W.; Dartiailh, C.; Cheng, J.; Charles, T. C.; Levin, D. B. Synthesis and Physical Properties of Polyhydroxyalkanoate Polymers with Different Monomer Compositions by Recombinant Pseudomonas Putida LS46 Expressing a Novel PHA SYNTHASE (PhaC116) Enzyme. *Appl. Sci.* **2017**, *7* (3). https://doi.org/10.3390/app7030242.

(57) Arrieta, M. P.; López, J.; Hernández, A.; Rayón, E. Ternary PLA-PHB-Limonene Blends Intended for Biodegradable Food Packaging Applications. *Eur. Polym. J.* **2014**, *50* (1), 255–270. https://doi.org/10.1016/j.eurpolymj.2013.11.009.

(58) Kopinke, F. D.; Remmler, M.; Mackenzie, K. Thermal Decomposition of Biodegradable Polyesters - I: Poly(β-Hydroxybutyric Acid). *Polym. Degrad. Stab.* **1996**, *52* (1), 25–38. https://doi.org/10.1016/0141-3910(95)00221-9.

(59) Grassie, N.; Murray, E. J.; Holmes, P. A. The Thermal Degradation of Poly(-(d)-β-Hydroxybutyric Acid): Part 1-Identification and Quantitative Analysis of Products. *Polym. Degrad. Stab.* **1984**, *6* (1), 47–61. https://doi.org/10.1016/0141-3910(84)90016-8.

(60) Vu, D. H.; Åkesson, D.; Taherzadeh, M. J.; Ferreira, J. A. Recycling Strategies for Polyhydroxyalkanoate-Based Waste Materials: An Overview. *Bioresour. Technol.* **2020**, *298* (September 2019). https://doi.org/10.1016/j.biortech.2019.122393.

(61) Pittmann, T.; Steinmetz, H. Polyhydroxyalkanoate Production on Waste Water Treatment Plants: Process Scheme, Operating Conditions and Potential Analysis for German and European Municipal Waste Water Treatment Plants. *Bioengineering* **2017**, *4* (2), 1–24. https://doi.org/10.3390/bioengineering4020054.

(62) Al Battashi, H.; Al-Kindi, S.; Gupta, V. K.; Sivakumar, N. Polyhydroxyalkanoate (PHA) Production Using Volatile Fatty Acids Derived from the Anaerobic Digestion

of Waste Paper. *J. Polym. Environ.* **2021**, *29* (1), 250–259. https://doi.org/10.1007/s10924-020-01870-0.

(63) Dinesh, G. H.; Nguyen, D. D.; Ravindran, B.; Chang, S. W.; Vo, D. V. N.; Bach, Q. V.; Tran, H. N.; Basu, M. J.; Mohanrasu, K.; Murugan, R. S.; Swetha, T. A.; Sivapraksh, G.; Selvaraj, A.; Arun, A. Simultaneous Biohydrogen (H2) and Bioplastic (Poly-β-Hydroxybutyrate-PHB) Productions under Dark, Photo, and Subsequent Dark and Photo Fermentation Utilizing Various Wastes. *Int. J. Hydrogen Energy* **2020**, *45* (10), 5840–5853. https://doi.org/10.1016/j.ijhydene.2019.09.036.

(64) García Prieto, C. V.; Ramos, F. D.; Estrada, V.; Villar, M. A.; Diaz, M. S. Optimization of an Integrated Algae-Based Biorefinery for the Production of Biodiesel, Astaxanthin and PHB. *Energy* **2017**, *139*, 1159–1172. https://doi.org/10.1016/j.energy.2017.08.036.

For Table of Contents Use Only

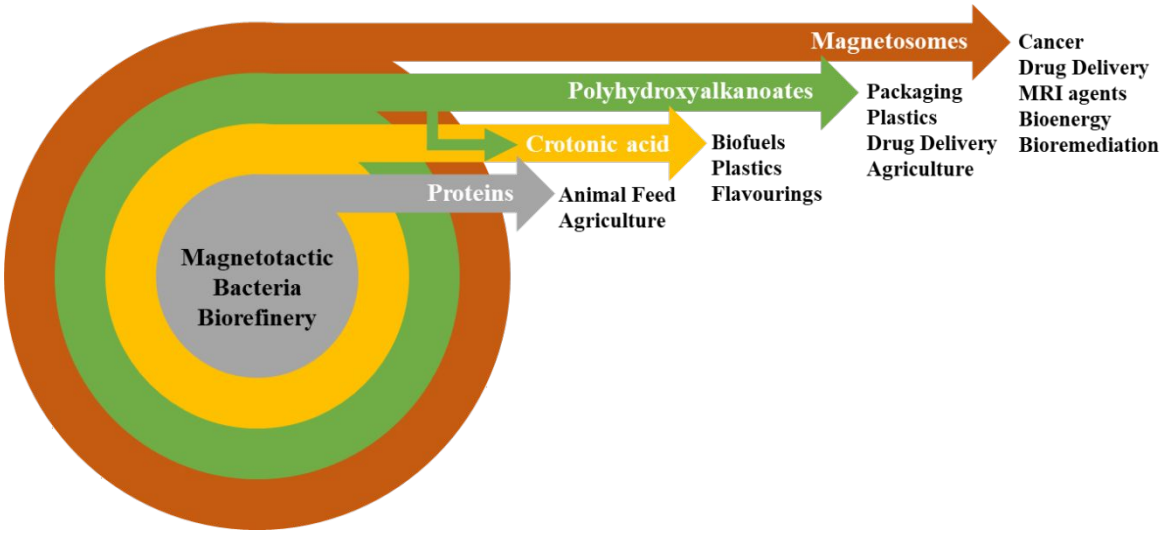


SYNOPSIS

Magnetotactic bacteria can be used not only for magnetosome production but also as source of other bio-chemicals that can be obtained through the use of green processing technologies.